Earth and Planetary Science Letters 310 (2011) 293–302

Contents lists available at SciVerse ScienceDirect

Earth and Planetary Science Letters

journal homepage: www.elsevier.com/locate/epsl

Effects of the Fe^{3+} spin transition on the properties of aluminous perovskite—New insights for lower-mantle seismic heterogeneities

Krystle Catalli [a,*], Sang-Heon Shim [a], Przemyslaw Dera [b], Vitali B. Prakapenka [b], Jiyong Zhao [c], Wolfgang Sturhahn [c,1], Paul Chow [d], Yuming Xiao [d], Hyunchae Cynn [e], William J. Evans [e]

[a] Department of Earth, Atmospheric and Planetary Sciences, Massachusetts Institute of Technology, Cambridge, MA 02139, USA
[b] GeoSoilEnviroCARS, University of Chicago, Argonne National Laboratory, Argonne, IL 60439, USA
[c] Sector 3, Advanced Photon Source, Argonne National Laboratory, Argonne, IL 60439, USA
[d] HPCAT, Advanced Photon Source, Argonne National Laboratory, Argonne, IL 60439, USA
[e] Lawrence Livermore National Laboratory, 7000 East Ave, Livermore, CA 94550, USA

ARTICLE INFO

Article history:
Received 6 May 2011
Received in revised form 21 July 2011
Accepted 11 August 2011
Available online 29 September 2011

Editor: L. Stixrude

Keywords:
Spin transition
Ferric iron
Aluminum
Heterogeneities
Perovskite

ABSTRACT

We have measured the effects of the coupled substitution of Fe^{3+} and Al on the density and compressibility of mantle silicate perovskite (Pv) up to 95 GPa. X-ray emission spectroscopy and synchrotron Mössbauer spectroscopy reveal a rapid increase in the population of low-spin Fe^{3+} in Fe^{3+}, Al-bearing Pv over a narrow pressure range near 70 GPa, which is in sharp contrast with Al-free Fe^{3+}-bearing Pv, where Fe^{3+} undergoes a gradual spin transition, and with Al-free Fe^{2+}-bearing Pv, where Fe^{2+} does not become low spin. At low pressure, Fe^{3+} and Al expand the perovskite lattice. However, near the pressure range of the abrupt increase in the low-spin population, the unit-cell volume of Fe^{3+}, Al-bearing Pv becomes similar to that of Mg-endmember Pv, while those of Al-free Fe^{3+}-bearing Pv and Al-free Fe^{2+}-bearing Pv remain larger throughout the lower mantle. Consequently, Pv in Al-rich systems should have lower density in the shallow lower mantle but similar or greater density than Pv in pyrolite in the deep lower mantle, affecting the buoyancy and mechanical stability of heterogeneities. Although the Fe^{3+} spin transition in Pv is unlikely to cause a seismic discontinuity at mantle temperatures, it may result in a large change in bulk sound speed at 1200–1800 km depth, such that a vertically extending structure with an elevated amount of Fe^{3+} would generate slower and faster anomalies above and below the depth of the spin transition, respectively, relative to the surrounding mantle. This may have important implications for bulk sound speed anomalies observed at similar depths in seismic tomography studies.

1. Introduction

Spin transitions in iron have been reported in the major lower-mantle minerals, magnesium silicate perovskite (Pv) and ferropericlase (Fp), at mantle pressures (Badro et al., 2003, 2004; Fei et al., 2007; Grocholski et al., 2009; Li et al., 2004; Lin et al., 2005, 2008; McCammon et al., 2008; Speziale et al., 2005; Tsuchiya et al., 2006; Umemoto et al., 2008). The spin transition in Fp, (Mg,Fe)O, has been found to induce a volume collapse to that of the magnesium endmember (i.e., MgO), resulting in a density increase at lower-mantle pressures (Fei et al., 2007; Lin et al., 2005; Speziale et al., 2005). However, Fp is expected to be a relatively minor component in the lower mantle while Pv makes up approximately 80%; thus the properties of Pv should significantly influence the bulk lower mantle.

Badro et al. (2004) reported a decrease in spin moment of iron in Pv at high pressure. Recent studies proposed a high spin to intermediate spin transition in Fe^{2+} at high pressure (Lin et al., 2008; McCammon et al., 2008), while other experimental (Grocholski et al., 2009) and computational (Bengtson et al., 2008; Stackhouse et al., 2007; Zhang and Oganov, 2006) studies have proposed that Fe^{2+} in Pv remains high spin throughout most of the lower mantle. Regardless, Lundin et al. (2008) showed that Fe^{2+} does not affect the pressure–volume relationship in Pv.

Mantle silicate perovskite is expected to contain 5–10% each of Fe and Al in the lower mantle (Kesson et al., 1998). Its crystal chemistry is complicated by the presence of two different crystallographic sites (dodecahedral, hereafter A, and octahedral, hereafter B, sites) available for cation substitution (Horiuchi et al., 1987). Iron may exist as both Fe^{2+} and Fe^{3+} with some studies finding up to 60% of iron to be Fe^{3+} in the presence of Al, even under reducing conditions (Frost et al., 2004; McCammon, 1997). Both theoretical (Hsu et al., 2011; Stackhouse

* Corresponding author.
E-mail address: krystle@alum.mit.edu (K. Catalli).
[1] Present address: Jet Propulsion Laboratory, 4800 Oak Grove Dr, Pasadena, CA 91109, USA.

0012-821X/$ – see front matter © 2011 Elsevier B.V. All rights reserved.
doi:10.1016/j.epsl.2011.08.018

et al., 2007) and experimental (Catalli et al., 2010; Xu et al., 2001) studies demonstrated that Fe^{3+} in the B site of Al-free Pv undergoes a high spin to low spin transition at much lower pressure than Fe^{2+}. The Mössbauer parameters and the spin transition of Fe^{3+} reported by Catalli et al. (2010) have been reproduced and confirmed by a recent first-principles study (Hsu et al., 2011).

The complex crystal chemistry of perovskite diversifies the environments for iron and complicates the interpretation of high pressure spectroscopy results, which have been inconsistent with one another (Badro et al., 2004; Grocholski et al., 2009; Li et al., 2004; Lin et al., 2008; McCammon et al., 2008). X-ray emission spectroscopy (XES) provides a measure of integrated spin population but does not distinguish iron in different valence states. Mössbauer spectroscopy is sensitive to both the valence and spin states of iron, but the interpretation of multiple iron sites in various states is difficult. The above issues can, therefore, be best resolved by measuring the effects of individual cations (Fe^{2+}, Fe^{3+}, and Al) on the properties of Pv with a combination of different spectroscopic techniques.

We have systematically studied the effects of different cations on the pressure–volume relationship of Pv, including pure magnesium endmember (Mg-Pv) (Lundin et al., 2008), with 9 and 15 mol% $FeSiO_3$ (Fe^{2+}-Pv) (Lundin et al., 2008), with 9 mol% Fe_2O_3 (Fe^{3+}-Pv) (Catalli et al., 2010), with 10 mol% Al_2O_3 (Al-Pv), and with 10 mol% $FeAlO_3$ (Fe^{3+}Al-Pv) (the latter two are reported here). All systems have been studied using the same pressure scale (gold) and pressure medium (argon) to allow for direct comparison between the different compositions. Therefore, these data sets provide important information on the effects of compositional variation on the density ($d\ln\rho/dX$) and bulk sound speed ($d\ln V_\phi/dX$) of Pv. Here we report synchrotron Mössbauer spectroscopy (SMS), XES, and X-ray diffraction (XRD) on Fe^{3+}Al-Pv in the laser-heated diamond cell to 95 GPa to measure the spin state of Fe^{3+} and its effect on the pressure–volume relationship in aluminous Pv. We discuss the effects of the Fe^{3+} spin transition in Pv on lower mantle structure and dynamics.

2. Experimental procedure

Glass starting materials ($0.90MgSiO_3 \cdot 0.05Al_2O_3 \cdot 0.05Fe_2O_3$ and $0.90MgSiO_3 \cdot 0.10Al_2O_3$, numbers are in mol fraction) were synthesized by the containerless laser levitation method (Tangeman et al., 2001). For the Fe^{3+}Al-Pv glass, synthesis was conducted under an O_2 atmosphere in order to prevent reduction during melting. By only allowing one valence state of iron (Fe^{3+}), the interpretation of SMS and XES data can be considerably simplified. Electron microprobe measurements revealed that the starting material is homogeneous and has a composition of $(Mg_{0.88}Fe_{0.13}Al_{0.11}Si_{0.88})O_3$ (± 0.01). The iron-bearing starting material is enriched with 95% ^{57}Fe for SMS.

The glass starting materials were ground to a powder and mixed with 10 wt.% gold for use as an internal pressure standard (Tsuchiya, 2003) for the XRD studies. For SMS and XES, ruby grains were placed at the edge of the sample chamber for pressure determination (Mao et al., 1986) instead of mixing with gold. For XRD and SMS, the sample powder was pressed to a foil and loaded into a preindented Re gasket. Argon was cryogenically loaded into the diamond cell, acting as both an insulating and a pressure medium, with a few spacer grains of sample material separating the sample foil from the diamond. For XES, 3 mm diameter Be gaskets with an initial central thickness of 100 μm were used. A sample platelet was pre-pressed and sandwiched between 5 μm layers of dried NaCl and loaded into the gasket hole.

Symmetric-type diamond anvil cells equipped with 200 or 300 μm culet diamonds were used for measurements with a peak pressure of less than 75 GPa, while 100 or 150 μm beveled culets were used above this pressure. Measurements on Fe^{3+}Al-Pv were taken from multiple sample loadings.

The perovskite phase was synthesized by double-sided laser heating at 2000 K for 30 min above 45 GPa using an Nd:YLF laser (Prakapenka et al., 2008). In addition, at each pressure the sample was scanned with the laser at 1800–2100 K for 7–15 min to synthesize the stable structure at the new pressure and to anneal deviatoric stress.

Angle-dispersive XRD was performed at the GSECARS sector of the Advanced Photon Source (APS) (Fig. 1). A monochromatic X-ray beam was focused to $5\times5\ \mu m^2$ with energy of 40 keV for measurements on Fe^{3+}Al-Pv and $10\times20\ \mu m^2$ at 30 keV for Al-Pv. Diffraction was collected using a MarCCD detector for Fe^{3+}Al-Pv and a Mar345 imaging plate for Al-Pv. Diffraction lines of argon in all diffraction patterns confirm the presence of the pressure/insulation medium. Both the hexagonal close-packed (hcp) and face-centered cubic structures are observed in some diffraction patterns (Fig. 1), likely due to the inclusion of a small amount of nitrogen during cryogenic loading of Ar, which stabilizes the hcp phase (Catalli et al., 2008; Wittlinger et al., 1997).

SMS was performed at the HPCAT and XOR-3 sectors of the APS (Fig. 2). At XOR-3, the 14.4 keV beam was focused to an area of $6\times6\ \mu m^2$. The storage ring was operated in top-up mode with 24 bunches separated by 153 ns. Nuclear resonant scattering was measured in a time window of 15–130 ns following excitation. Data collection typically took 2–4 h (see Jackson et al., 2005; Sturhahn and Jackson, 2007; Catalli et al., 2010, for details). At beamline 16-IDD of HPCAT, the beam size was $30\times40\ \mu m^2$ and data collection time was 8–10 h. SMS data were fit using the CONUSS package (Sturhahn, 2000) (Fig. 3).

XES was performed at the HPCAT sector of APS (Fig. 4). An 11.35 keV X-ray beam was focused down to $30\times40\ \mu m^2$ on the sample. Emission was collected through the Be gasket. Collection time was typically 8–16 h. The spectra have been aligned relative to a reference spectrum (iron foil) according to their centers of mass

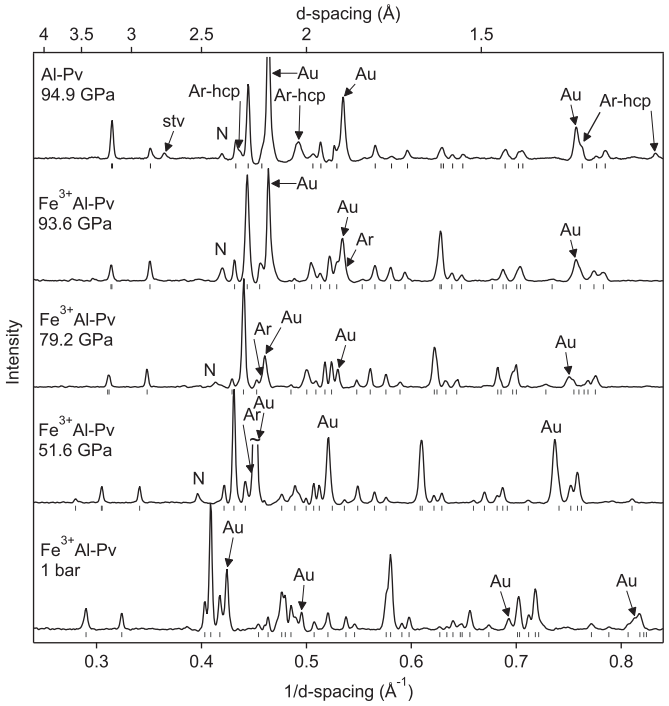

Fig. 1. Representative X-ray diffraction patterns of Fe^{3+}Al-Pv (bottom four patterns) and Al-Pv (topmost pattern). The ticks below each diffraction pattern show the locations of perovskite lines used for the calculation of volume and lattice parameters. Au: gold; Ar: argon; Ar-hcp: hcp structured argon; stv: stishovite; N: nitrogen. Backgrounds have been subtracted.